ARTICLE IN PRESS

Available online at www.sciencedirect.com

SCIENCE DIRECT®

Biomaterials ▮ (▮▮▮▮) ▮▮▮–▮▮▮

Biomaterials

www.elsevier.com/locate/biomaterials

Cytotoxicity suppression and cellular uptake enhancement of surface modified magnetic nanoparticles

Ajay Kumar Gupta[a,*], Mona Gupta[b]

[a] Centre for Cell Engineering, Institute of Biomedical and Life Sciences, Joseph Black Building, University of Glasgow, Glasgow G12 8QQ, Scotland, UK

[b] Division of Biochemistry and Molecular Biology, Institute of Biomedical and Life Sciences, University of Glasgow, Glasgow G12 8QQ, Scotland, UK

Received 18 March 2004; accepted 12 May 2004

Abstract

The aim of this study was to modify the surfaces of superparamagnetic iron oxide nanoparticles (SPION) with pullulan in order to reduce the cytotoxicity and enhance the cellular uptake of the nanoparticles. In this study, we have prepared and characterised the pullulan coated superparamagnetic iron oxide nanoparticles (Pn-SPION) of size around 40–45 nm with magnetite inner core and hydrophilic outer shell of pullulan. We have investigated the effect of cellular uptake of uncoated and Pn-SPION on cell adhesion/viability, cytotoxicity, morphology and cytoskeleton organisation of human fibroblasts. Cell cytotoxicity/adhesion studies of SPIONs on human dermal fibroblasts showed that the particles are toxic and their internalisation resulted in disruption of cytoskeleton organisation of cells. On the other hand, Pn-SPIONs were found to be non-toxic and induced changes in cytoskeleton organisation different from that observed with SPION. Transmission electron microscopy results indicated that the SPION and Pn-SPION were internalised into cells via different mechanisms, thereby suggesting that the particle endocytosis behaviour is dependent on the surface characteristics of the nanoparticles.

Keywords: Drug delivery; Magnetic nanoparticle; Surface modification; Cell adhesion; TEM; Cytotoxicity

1. Introduction

Superparamagnetic iron oxide nanoparticles have been recognised as a promising tool for the site-specific delivery of drugs and diagnostics agents [1,2]. Magnetic properties and internalisation of particles in cells depend strongly on the size of the magnetic particles [3]. Particles below 100 nm are small enough both to evade reticuloendothelial system (RES) of the body as well as penetrate the very small capillaries within the body tissues [4]. Because of their hydrophobic surfaces and large surface area to volume ratio, in vivo use of nanoparticles is hampered by very rapid clearance of nanoparticles from the circulation by the RES. Avoidance of this obstacle is possible if the surfaces of these nanoparticles are made sufficiently hydrophilic, as these modifications prolong considerably the nanoparticle half-life in the circulation [5].

Surface characteristic of nanoparticles is a crucial factor that not only determines the biocompatibility of these magnetic materials but also plays an important role in cell adhesion on biomaterials [6,7]. Adhesive interactions between cells and the extracellular matrix (ECM) or particles are governed primarily by integrins, a large family of cell surface adhesion receptors [8,9]. Integrin-mediated cell adhesion is central to cell survival, differentiation and motility and is known to activate focal adhesion kinase (FAK), which plays a role in cytoskeleton reorganisation [10]. In addition, earlier we have shown that the event of endocytosis occurs by the reorganisation of cell cytoskeleton [11,12]. This is because of the fact that the elastic properties of a cell are mainly due to the internal cytoskeleton consisting of

*Corresponding author. Crusade Laboratories Limited, Southern General Hospital, 1345, Govan Road, Glasgow G51 4TF, UK. Tel.: +44-141-445-1716; fax: +44-141-445-1715.

E-mail addresses: agupta@crusadelabs.co.uk, akgupta25@hotmail.com (A.K. Gupta).

0142-9612/$ - see front matter © 2004 Elsevier Ltd. All rights reserved.
doi:10.1016/j.biomaterials.2004.05.022

three types of filamentous proteins: actin, microtubules and intermediate filaments, etc. [13]. The cytoskeleton plays a major role in many important fields such as cell shape, motility, division, adhesion and the connections the cell can realise with its environment [14]. Also there is a link between cytoskeleton components and endocytosis. Relation between the two processes is highly dynamic and may involve interactions between distinct protein complexes, depending on the nature of the cargo being internalised [15]. As a result, there could be different kind of changes in proteins responsible for maintaining cytoskeleton organisation, which may ultimately result from different pathways of particle internalisation. The nature and adhesion capacity of cells in the presence of nanoparticles as well as the subsequent cellular events such as endocytosis and changes in cytoskeleton organisation have not been fully elucidated yet.

Therefore, the objectives of this study were to prepare and characterise the surface modified superparamagnetic iron oxide nanoparticles (both SPION and Pn-SPION) and determine (i) the adhesion capacity, (ii) endocytosis behaviour and (iii) effect on cytoskeleton organisation of human fibroblasts as a result of nanoparticle internalisation. Pullulan, a nonionic polysaccharide, was chosen as a coating material for SPION due to the following properties: (i) high water solubility, (ii) no toxicity, (iii) usefulness as a plasma expander, (iv) non-immunogenic and (v) non-antigenic properties [16]. Also, pullulan is widely used as a food additive because of its safety in human use (http://www2.minlnv.nl/lnv/algemeen/vvm/codex/documenten/2003/CCFAC/fa36_36e.pdf). In addition, there are evidences for receptor-mediated hepatic uptake of pullulan in rats [17]. The influence of Pn-SPION on human fibroblasts in vitro has been determined as compared to SPION, in terms of cell adhesion/cytotoxicity, TEM and observation of *F*-actin and β-tubulin cytoskeleton by fluorescence microscopy.

2. Materials and methods

2.1. Materials

Ferric chloride hexahydrate ($FeCl_3 \cdot 6H_2O > 99\%$), ferrous chloride tetrahydrate ($FeCl_2 \cdot 4H_2O$), pullulan, potassium thiocyanate (ACS reagent $\geqslant 99.0\%$), ammonium persulphate (ACS reagent, $\geqslant 99.0\%$) and 3-(4,5-dimethylthiazol-2-yl)-2,5-diphenyltetrazolium bromide (MTT) were obtained from Sigma, England, UK, while sodium hydroxide ($NaOH > 99\%$) and hydrochloric acid ($HCl > 37\%$ v/v) were obtained from Fluka, England, UK. Double distilled water was used for all the experiments.

2.2. Synthesis of Pn-SPION

Magnetic nanoparticles, SPION, were synthesised by co-precipitation of ferrous and ferric salts solution by concentrated sodium hydroxide solution inside the aqueous cores of reverse micelles as reported previously [18]. Pullulan was coated onto the nanoparticles surface in order to increase the stability of the particles under in vitro and in vivo conditions. Briefly, 100 mg magnetite particles were dispersed in 10 ml of deoxygenated water by sonication (50 W, 30 min). To this solution, 10 ml of 1% w/v of pullulan aqueous solution was added. Five hundred microliters (1.0% v/v) of glutaraldehyde was added to this solution to cross-link the individual polymeric chains of pullulan. The reaction was carried out for 4 h at 37°C under nitrogen gas with continuous stirring. Particles were then purified by dialysis for 6 h using 12 kD cut off dialysis membrane against double distilled water. The aqueous suspension of the nanoparticles was freeze-dried before characterisation.

2.3. Characterisation of magnetic nanoparticles

2.3.1. Fourier transformed infrared (FTIR) spectral studies

The FTIR spectrum was recorded in the transmission mode on a Nicolet Impact 410 spectrometer. The dried samples of SPION or Pn-SPION were grounded with KBr and mixture was compressed into a pellet. The spectrum was taken from 4000 to 400 cm^{-1}.

2.3.2. Transmission electron microscopy (TEM) studies

The average particle size, size distribution and morphology of SPION and Pn-SPION were examined using a Zeiss 902 transmission electron microscope at a voltage of 80 kV. The aqueous dispersion of the particles was drop-cast onto a carbon-coated copper grid and the grid was air dried at room temperature before viewing under the microscope.

2.3.3. Atomic force microscopy (AFM) studies

The aqueous dispersion of the nanoparticles was put on a glass coverslip and the coverslip was dried in a vacuum desiccator. Once dry, the samples were analysed using The Nanoscope® III Scanning Probe Microscope (Digital Instruments, Santa Barbara, California, USA).

2.3.4. Total iron determination

In order to absorb certain wavelengths it is necessary for the given species to be coloured. Metals such as iron form highly coloured complexes when reacted with the thiocyanate ion [19]:

$$Fe^{3+}_{(aq)} + 6SCN^{-}_{(aq)} \rightarrow [Fe(SCN)_6]^{3-}_{(aq)}.$$

The iron present in the nanoparticles was extracted by completely dissolving the 10 mg nanoparticles in 10 ml of 30% v/v HCl for 2 h at 50–60°C. A total of 1.0 mg of ammonium persulphate was then added to oxidise the ferrous ions present in the above solution to ferric ions. In all, 1.0 ml of 0.1 M solution of potassium thiocyanate was added to this solution to form the iron-thiocyante complex. The iron concentration was determined by spectrophotometric measurements at 478 nm using a Shimadzu UV-160A UV-visible recording spectrophotometer. A standard curve for the iron was made under identical conditions using known amount of iron salts.

2.4. Cytotoxicity and cellular uptake of magnetic nanoparticles

2.4.1. Cell culture

Infinity^{TM} telomerase-immortalised primary human fibroblasts (hTERT-BJ1, Clontech Laboratories Inc., England, UK) were chosen for cell culture experiments, as these fibroblasts are highly stable, fast growing and represent well-defined internal cytoskeleton components [20]. The medium used was 71% Dulbecco's modified Eagle's medium (DMEM) (Sigma, England), 17.5% Medium 199 (Sigma, Dorset, England, UK), 9% foetal calf serum (FCS) (Life Technologies Ltd., Paisley, Scotland, UK), 1.6% 200 mM L-glutamine (Life Technologies Ltd., UK), and 0.9% 100 mM sodium pyruvate (Life Technologies Ltd., UK). The cells were incubated at 37°C in a 5% CO_2 atmosphere.

2.4.2. In vitro cell viability/cytotoxicity studies

To determine cell cytotoxicity/ viability, the cells were plated at a density of 1×10^4 cells/well in 96 well plate at 37°C in 5% CO_2 atmosphere. After 24 h of culture, the medium in the wells was replaced with the fresh medium containing nanoparticles (SPION or Pn-SPION) in concentration range 0–2.0 mg/ml. After 24 h, 20 μl of MTT dye solution (5 mg/ml in phosphate buffer pH-7.4) was added to each well. After 4 h of incubation at 37°C, the medium was removed and formazan crystals were solubilised with 200 μl of dimethylsulphoxide (DMSO) and the solution was vigorously mixed to dissolve the reacted dye. After 15 min, the absorbance of each well was read on a microplate reader (DYNATECH MR7000 instruments) at 570 nm. The spectrophotometer was calibrated to zero absorbance, using culture medium without cells. The relative cell viability (%) related to control wells containing cell culture medium without nanoparticles was calculated by $[A]_{test}/[A]_{control} \times 100$.

Where $[A]_{test}$ is the absorbance of the test sample and $[A]_{control}$ is the absorbance of control sample.

2.4.3. Cell adhesion assay

The effect of nanoparticles on cell adhesion was determined with cell suspension incubated with or without nanoparticles. Fibroblasts were expanded in monolayer tissue culture. The cells were detached using trypsin-EDTA solution and divided into two individual populations. Cells were seeded with or without nanoparticles at concentration 0.5 mg/ml for 24 h onto coverslips (13 mm diameter; in triplicate) at 37°C in 5% CO_2. At the end of 24 h, the cells were rinsed thrice with phosphate buffered saline, fixed in situ with 4% formaldehyde/PBS (15 min, 37°C), and stained for 2 min with 1% Coomassie Blue in acetic acid. Stained cells in five random fields were counted using light microscopy and the digital images of the fibroblasts were captured using a Hamamatsu Argus 20 camera. Results were represented as mean ± SD.

2.4.4. Immunofluorescence and cytoskeleton organisation

After 24 h of culture the cells with the nanoparticles (0.1 mg/ml) along with controls were fixed in 4% formaldehyde/PBS, with 1% sucrose at 37°C for 15 min, to allow the viewing of individual cells. When fixed, the samples were washed with PBS, and a permeabilising buffer (10.3 g of sucrose, 0.292 g of NaCl, 0.06 g of $MgCl_2$, 0.476 g of Hepes buffer, 0.5 ml of Triton X, in 100 ml of water, pH 7.2) was added at 4°C for 5 min. The samples were then incubated at 37°C for 5 min in 1% BSA/PBS. This was followed by the addition of anti-β tubulin primary antibody (1:100 in 1% BSA/PBS, Sigma, Poole, UK) for 1 h (37°C). Simultaneously, rhodamine-conjugated phalloidin was added for the duration of this incubation (1:100 in 1% BSA/PBS, Molecular Probes Inc., Eugene, OR). The samples were next washed in 0.5% Tween 20/PBS (5 min × 3). A secondary, biotin-conjugated antibody (1:50 in 1% BSA/PBS, monoclonal horse antimouse (IgG), Vector Laboratories Ltd., Peterborough, England, UK) was added for 1 h (37°C) followed by washing. A FITC conjugated streptavidin tertiary antibody was added (1:50 in 1% BSA/PBS, Vector Laboratories Ltd., UK) at 4°C for 30 min, and given a final wash. Samples were mounted in Vectorshield fluorescent mountant (Vector Laboratories Ltd., UK), and then viewed by fluorescence microscope (Vickers M17). The imaging system used was a Hamamatsu Argus 20 with an × 7 Hamamatsu CCD camera.

2.4.5. Transmission electron microscopy

The fibroblasts were seeded onto 13-mm glass coverslips in a 24 well plate at a density of 1×10^4 cells per well in 1 ml of complete medium for 24 h after which the growth medium was removed and replaced with the medium containing nanoparticles (0.1 mg/ml medium).

For control experiments, medium without nanoparticles was used. After 12 and 24 h of culture, the cells were fixed with 1.5% glutaraldehyde (Sigma, Dorset, England, UK) buffered in 0.1 M sodium cacodylate (Agar Scientific, Stansted Essex, England, UK) (4°C, 1 h). The cells were then post-fixed in 1% osmium tetroxide (Agar Scientific, Stansted Essex, England, UK), and 1% tannic acid (Agar Scientific, Stansted Essex, England, UK) was used as a mordanant. Samples were dehydrated through a series of alcohol concentrations (20%, 30%, 40%, 50%, 60%, 70%) followed by further dehydration (90%, 96%, 100% and dry alcohol). The cells were finally treated with propylene oxide followed by 1:1 propylene oxide:resin for overnight to evaporate the propylene oxide. The cells were subsequently embedded in Araldite resin, and ultra-thin sections (60 nm) cut with glass knives were stained with lead nitrate and viewed under a Zeiss 902 electron microscope at 80 kV.

2.4.6. Statistical analysis

Each experiment was repeated three times in duplicate. The statistical analysis of experimental data utilised the Student's *t*-test and the results were presented as mean ± SD. Statistical significance was accepted at a level of $p < 0.05$.

3. Results

3.1. Characterisation of magnetic nanoparticles

3.1.1. FTIR studies

Fig. 1 displays the FTIR spectra of solid samples of SPION and SPION modified by the pullulan (Pn-SPION). The FTIR spectra of iron oxide exhibit strong bands in the low frequency region below 800 cm^{-1} due to the iron oxide skeleton. In other regions, the spectra of iron oxide have weak bands. The spectrum is consistent with magnetite (Fe_3O_4) and the signals associated to the magnetite appear as broad features at 408.9, 571.5 and 584.5 cm^{-1} [18]. The main characteristic vibrations of the pullulan as coating material, the NH bending and C=O stretching modes are expected to appear around 1400 cm^{-1}. Comparing the FTIR spectra of SPION and those of Pn-SPION, one clearly sees bands near 1637, and 1413 cm^{-1}, which could be due to the pullulan coating. Also, the signals observed at 1020 and 1637 cm^{-1} are due to the C–CO and C=O stretching modes in polymer. The bands near 2928 and 955 cm^{-1} correspond to $–CH_2$ stretching vibrations and –CH out-of-plane bending vibrations, respectively. The N–H, C=O, $–CH_2$ and –CH peaks indicate that pullulan was covered at the nanoparticle surface.

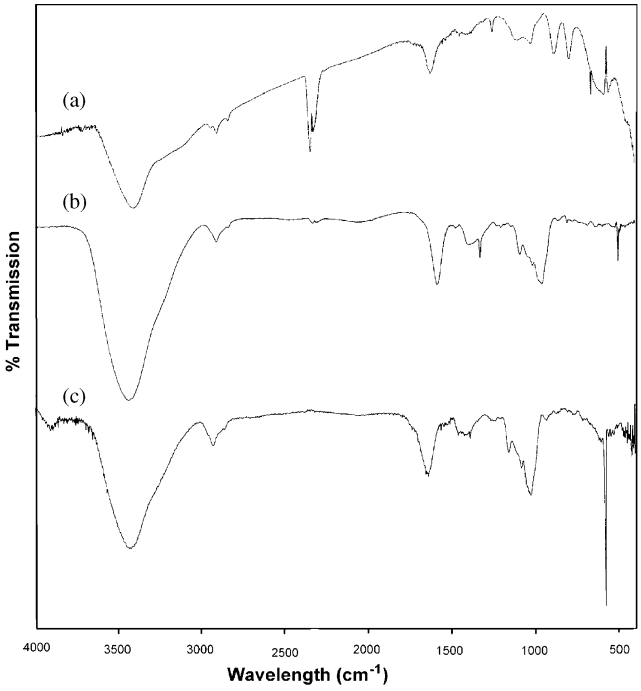

Fig. 1. FTIR spectra of (a) magnetic nanoparticles, SPION, and (b) pullulan, Pn, and (c) pullulan coated magnetic nanoparticles, Pn-SPION.

3.1.2. Size distribution studies by TEM and AFM measurements

Average size of the particles was determined by TEM by measuring the size of about 200 particles. Fig. 2(a) shows that the particles are cubic shaped with an approximate size of around 13.6 nm with a standard deviation of 0.78 nm. The size of the particles after coating was 42.0 ± 2.5 nm diameter (Fig 2(b)). AFM was performed to study the shape, size and core-shell structure of the nanoparticles. Fig. 3 represents the AFM image of Pn-SPION showing the core shell structure and size homogeneity of the nanoparticles. Average particle diameter of the particles was found about 45 nm, which is in agreement with the size obtained by TEM studies.

3.1.3. Total iron determination

Ferrous ions present in the solution were oxidised to ferric ions by ammonium persulphate prior to reacting with thiocyanate salt to form the iron-thiocyanate complex. Concentration of the complex and, hence, iron content in the nanoparticles was determined spectrophotometrically. Iron content in the nanoparticles was found to be more than 90% of the original iron salts. It was calculated that a total of 1.71×10^{17} particles are present in one gram of magnetic nanoparticles and each iron oxide nanoparticle contained 62896 iron atoms [18].

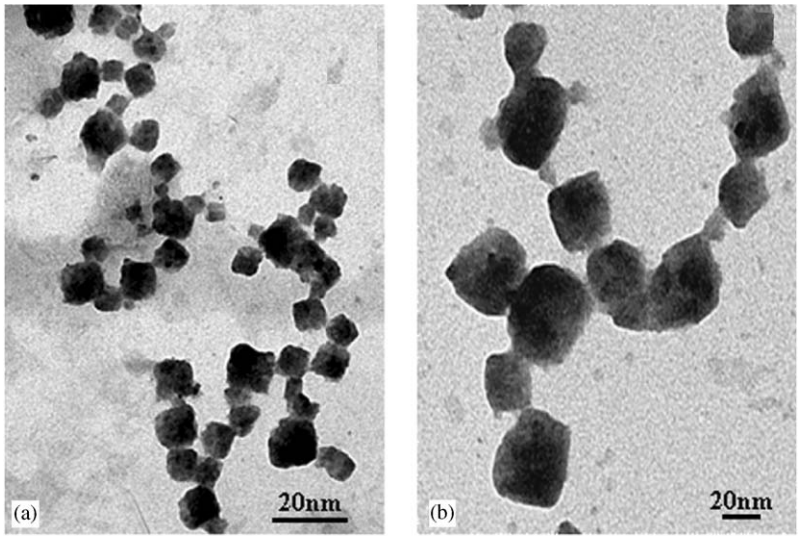

Fig. 2. Transmission electron microscopy pictures of (a) magnetic nanoparticles, SPION, and (b) pullulan coated magnetic nanoparticles, Pn-SPION.

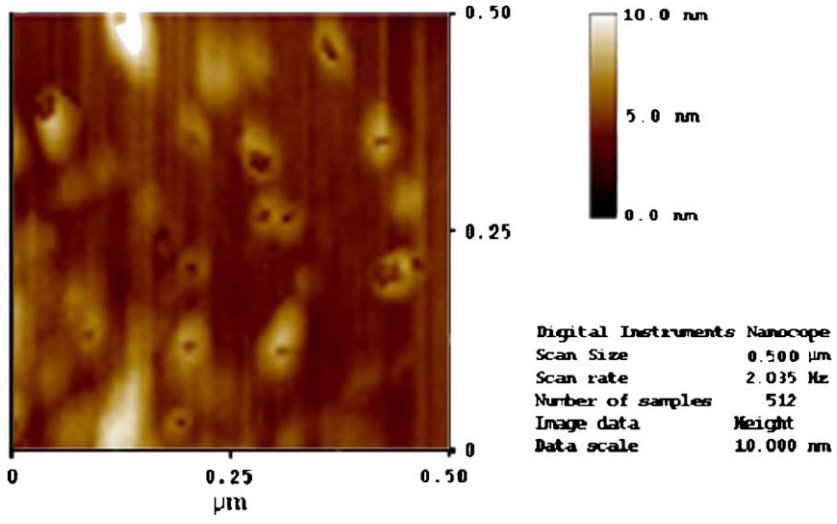

Fig. 3. Atomic force microscope picture showing core-shell structure of Pn-SPION. The particles have inner magnetite core and outer polymeric shell of pullulan.

3.2. Cytotoxicity and cellular uptake of magnetic nanoparticles

3.2.1. In vitro cell viability/cytotoxicity studies

Viable cells have the ability to reduce MTT from a yellow water-soluble dye to a dark blue insoluble formazan product [21]. Formazan crystals were dissolved in DMSO and quantified by measuring the absorbance of the solution at 570 nm, and the resultant value is related to the number of living cells. Fig. 4 demonstrated a dose-dependent reduction in MTT absorbance in cells treated with SPION (concentration range 0–2.0 mg/ml) for 24 h. SPION caused a significant reduction (80% of control) in cell viability even at the lowest concentration tested (0.05 mg/ml), and induced further reductions at higher concentrations, reaching a plateau around 0.5 mg/ml, and that at the highest concentration tested (2.0 mg/ml) it resulted in about 60% loss of cell viability. Pn-SPION showed no cytotoxic effects to cells and the cells remained more than 92% viable relative to control at concentration as high as 2.0 mg/ml.

3.2.2. Cell adhesion assay

The effect on cell adhesion capacity of fibroblasts on incubation with SPION and Pn-SPION for 24 h was determined as compared to control cells (without particles) and the results are shown in Fig. 5. The figure

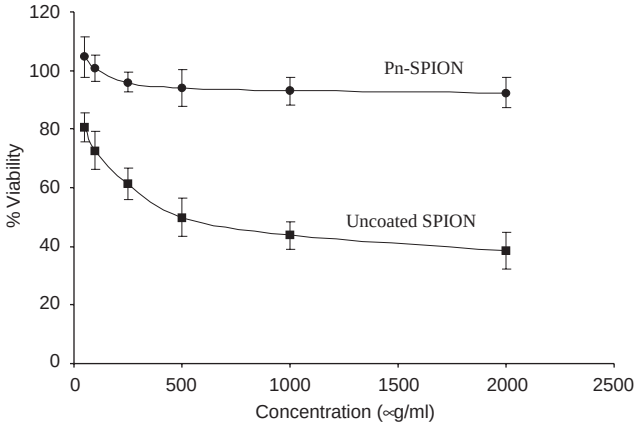

Fig. 4. Fig. 6. Cytotoxicity profiles of SPION and Pn-SPION, when incubated with human fibroblasts as determined by MTT assay. Percent viability of fibroblasts was expressed relative to control cells ($n = 6$). Results are represented as mean ± SD.

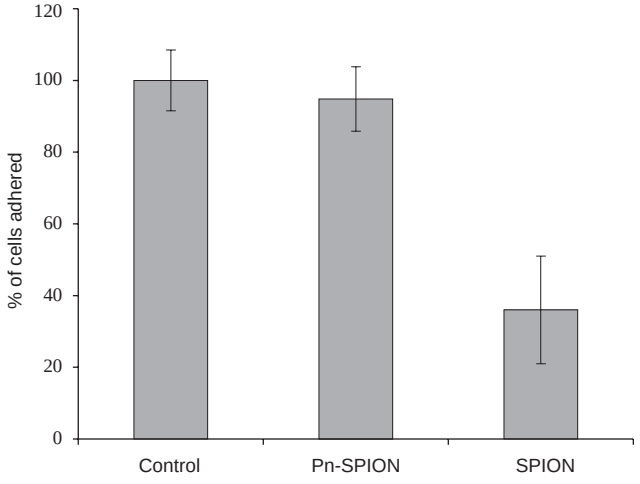

Fig. 5. Graphical representation of number of cells adhered, when incubated with SPION and Pn-SPION particles onto glass coverslips, after 24 h culture as compared to controls (results are represented as mean ± SD; $n = 3$; counted in triplicate in individual microscope fields).

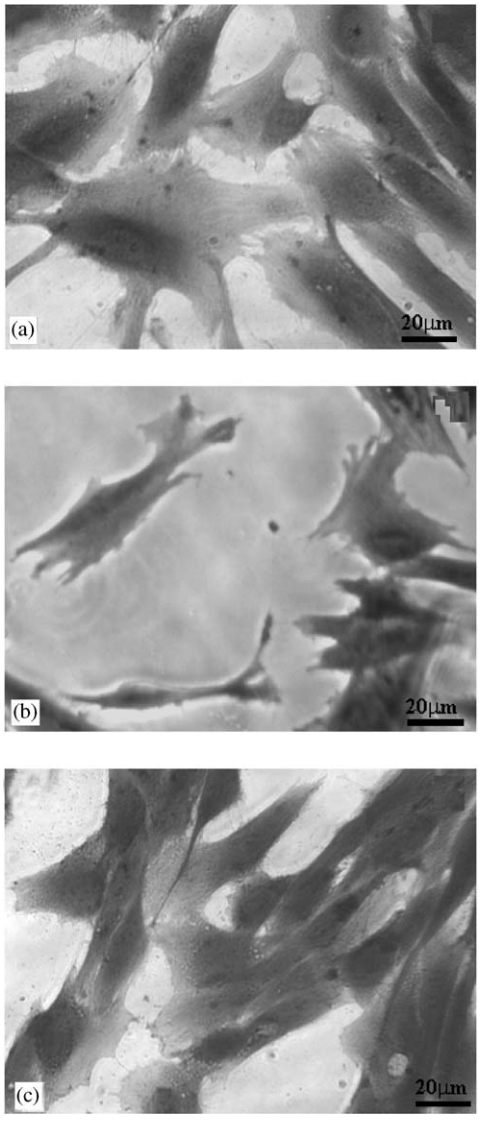

Fig. 6. Coomassie blue stained cells incubated with magnetic particles for 24 h at 37°C (a) control, (b) uncoated, (c) pullulan coated nanoparticles; $n = 3$.

shows that the number of attached cells was decreased significantly upto 64% in case of SPION compared to the corresponding control cell number. Growing the cells with Pn-SPION produced no significant difference compared to that of control cell population (Fig. 6).

3.2.3. *Immunofluorescence and cytoskeleton organisation*

To determine the effect of cellular uptake of Pn-SPION and SPION nanoparticles on cytoskeleton organisation of fibroblasts, *F*-actin and *β*-tubulin cytoskeleton components were stained using rhodamine-phalloidin for *F*-actin and anti-tubulin antibodies for *β*-tubulin (Fig. 7). Untreated cells exhibited strong peripheral *F*-actin staining along the cell edge, indicative of cortical actin fibres (Fig. 7). Also, the microfilaments were well organised in thick bundles forming stress fibres. The microtubules also form a dense network equally distributed around the nucleus of the cells. In the case of cells incubated with Pn-SPION, there were prominent stress fibres reflecting from the cell periphery as observed in the control cell. However, the addition of SPION exhibited smaller cell structures and also caused a rapid disruption of actin distribution within the cell. Also the incubation with the SPION resulted in disruption of microtubule structures in the central and peripheral domain of the fibroblasts compared to control cells. The effect of Pn-SPION treatment is demonstrated by the diffused tubulin staining and formation of cell protrusions, suggesting higher levels of free tubulin relative to control cells.

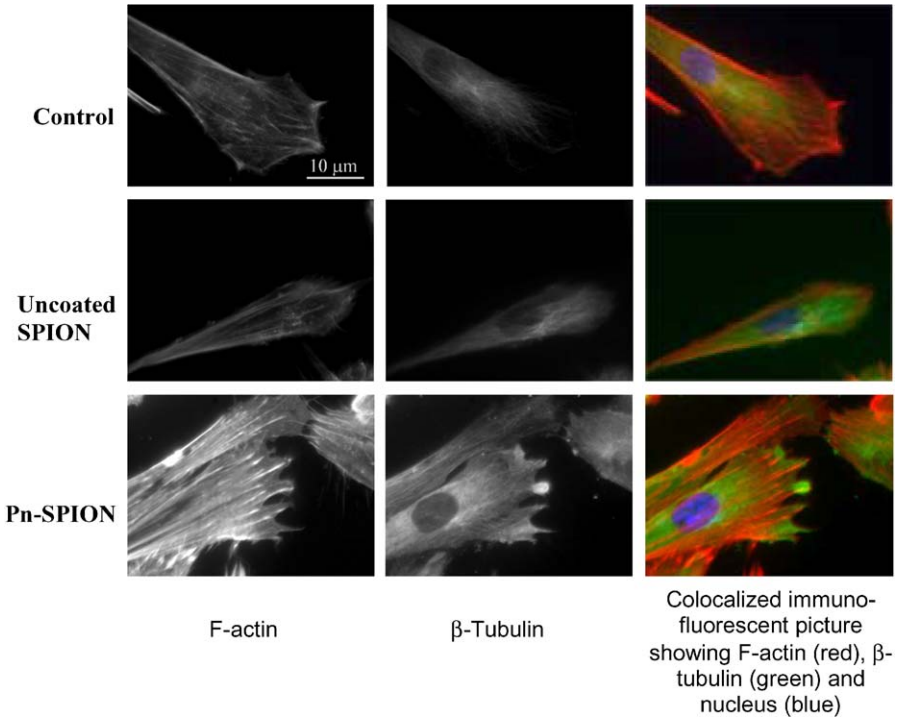

Fig. 7. Cells incubated with different coated particles and stained for β-tubulin (green), *F*-actin (red) and nucleus (blue) ($n = 3$).

3.2.4. Transmission electron microscopy

Differences in the uptake mechanism between the two nanoparticles types were confirmed by the transmission electron microscopy images taken at 12 and 24 h as shown in Fig. 8. The images showed that the SPION are internalised within the fibroblast after 12 and 24 h (Figs. 8a and b, respectively). Several electron lucent voids containing nanoparticles can be seen in the cytoplasm of the fibroblasts forming the vacuoles. As shown in Figs. 8c and d, after 12 h, some Pn-SPIONs could be seen adhered on the surfaces of the cells probably to the cell expressed surface receptors for pullulan molecules. Also few particles have been endocytosed at this stage by the fibroblasts (Fig. 8d). Thereafter, at 24 h (Fig. 8e), the nanoparticles are endocytosed probably via receptor-mediated endocytosis.

4. Discussion

The colloidal solution of Pn-SPION showed very high stability at neutral pH with no sedimentation observed even after 2 months of storage at room temperature. The strong anchoring of the pullulan molecules on the surface of iron oxide results in the steric stabilisation of the particles. Size distribution studies using TEM and AFM measurements showed that the particles have size less than 50 nm with inner magnetic core and outer polymeric shell (core-shell structure).

Cell adhesion/viability studies indicated that the SPION reduced cell adhesion/viability significantly ($p < 0.05$) as compared to the cells that were not exposed to the nanoparticles. One possible explanation for this large decrease in cell adhesion/viability may be that these nanoparticles are taken up by the cells as a result of endocytosis and promoting apoptosis due to weak cell adhesive interactions with the nanoparticles [22,23]. The low toxicity of Pn-SPION may be attributed to the fact that pullulan is hydrophilic, and it protects surfaces from interacting with cells or proteins.

From the results of cytoskeleton organisation studies, we observed that both types of nanoparticles induced different changes in cytoskeleton organisation, thereby suggesting that fibroblasts had utilised different mechanisms to internalise the particles. A probable reason for different uptake mechanism of nanoparticles is that there is a link between cytoskeleton organisation and endocytosis. Relation between the two processes involves interactions between distinct protein complexes, depending on the nature of the particles being internalised [15,24]. TEM studies indicated the differences in the particles uptake behaviour of the fibroblasts. These results indicate that although both types of nanoparticles are taken up by the cells, the Pn-SPIONs reduce cell cytotoxicity and induce cellular uptake behaviour distinct from the SPIONs, suggesting that particle endocytosis response is dependent on the particles

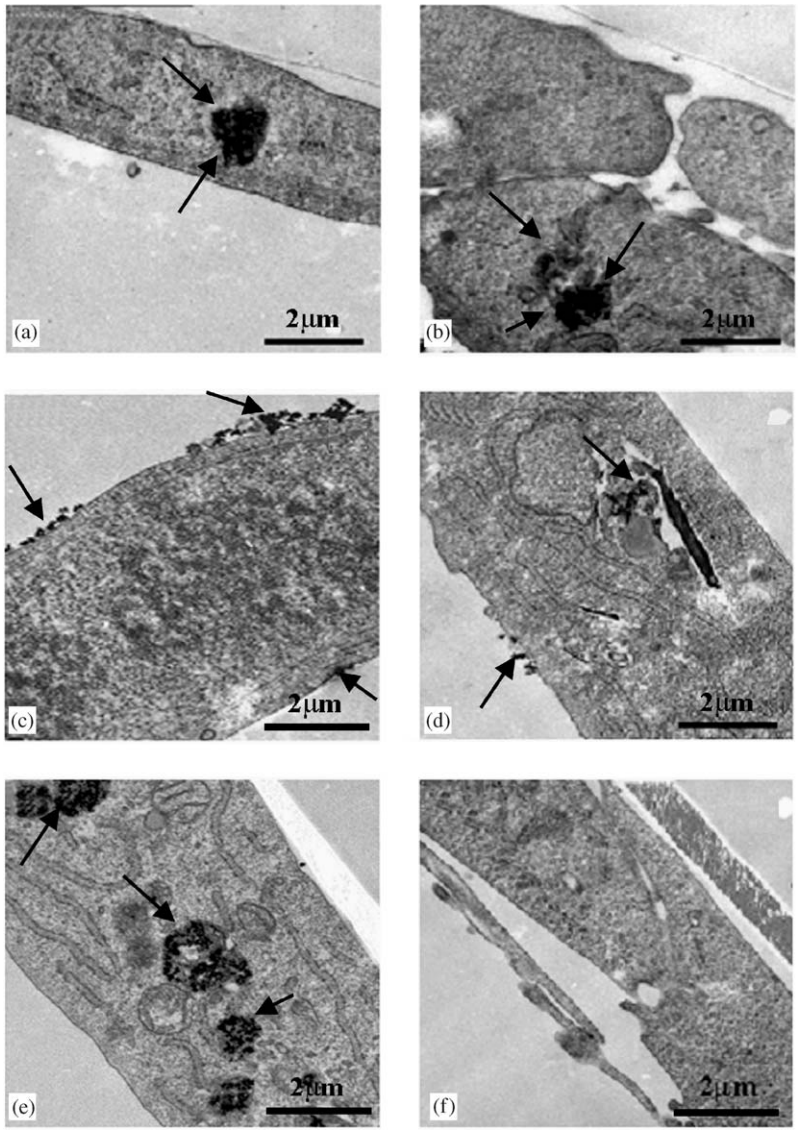

Fig. 8. TEM pictures of human fibroblasts incubated with (a, b) SPION showing nanoparticle internalisation after 12 and 24 h (a and b, respectively) (see arrows); (c-e) Pn-SPION showing nanoparticles at the cell surface after 12 h incubation (c and d) (see arrows); After 24 h (Fig. 7e) the particles were internalised inside the cells probably via receptor mediated endocytosis; and (f) control fibroblasts.

coating. In a study, Kaneo et al. [17] have shown the evidence for receptor-mediated hepatic uptake of pullulan in rats. Their results have indicated that the pullulan has high affinity for asialoglycoprotein receptors on hepatocytes. In another paper, Xi et al. [25] studied the targeting of interferon to the liver through chemical conjugation with pullulan. Pullulan modified iron oxide nanoparticles, however, may prove very useful for imaging of the vascular compartment (magnetic resonance angiography), imaging of lymph nodes, perfusion imaging, receptor imaging and target specific imaging. These findings suggest the possibility to deliver Pn-SPIONs into different tissues with high uptake efficiency has high potential in biotechnology.

5. Conclusions

In this paper, Pn-SPION of size about 40–50 nm having core-shell structure with magnetic core and polymeric shell have been prepared and characterised in vitro by various physicochemical means. The colloidal solution of nanoparticles showed high stability. The results of cell culture experiments have indicated that the Pn-SPIONs were non-toxic as comparing to SPIONs and because of the surface modification the cellular uptake of Pn-SPION could be enhanced. Pn-SPIONs were internalised by cells via a different route that was not involved with SPION endocytosis. Combined with existing advanced concepts of particulate drug delivery and magnetic therapy, pullulan-coated

magnetic particles may provide additional specificity and efficacy, which are required in many drug and gene therapy approaches.

Acknowledgements

The authors would like to thank Professor Adam S.G. Curtis, Centre for Cell Engineering, IBLS, University of Glasgow, Glasgow, UK for encouraging us to work in his laboratory. Thanks are also due to Mr. Eoin Robertson and Mrs. M. Mullin, EM Unit, Institute of Biomedical and Life Sciences, University of Glasgow, Glasgow, UK for their technical assistance.

References

[1] Weissleder R, Bogdanov A, Neuwelt EA, Papisov M. Long circulating iron oxides for MR imaging. Adv Drug Del Rev 1995;16:321–34.
[2] Berry CC, Curtis ASG. Functionalisation of magnetic nanoparticles for applications in biomedicine. J Phys D: Appl Phys 2003;36:R198–206.
[3] Chouly C, Pouliquen D, Lucet I, Jeune JJ, Jallet P. Development of superparamagentic nanoparticles for MRI: effect of particle size, charge and surface nature on biodistribution. J Microencapsul 1996;3:245–55.
[4] Moghimi SM, Hunter AC, Murray JC. Long circulating and target specific nanoparticles: theory to practise. Pharm Rev 2001;53:283–318.
[5] Stolnik S, Illum L, Davis SS. Long circulating microparticulate drug carriers. Adv Drug Del Rev 1995;16:195–214.
[6] Gupta AK, Curtis ASG. Lactoferrin and ceruloplasmin derivatized superpara-magnetic iron oxide nanoparticles: preparation, characterization and their influence on human dermal fibroblasts in culture. Proc Ann Symp Control Rel Bioact Mater 2003;30:788.
[7] Hallab NJ, Bundy KJ, O'Connor K, Clark R, Moses RL. Cell adhesion to biomaterials: correlations between surface charge, surface roughness, adsorbed protein and cell morphology. J. Long-Term Eff Med Implants 1995;5(3):209–31.
[8] Absolom DR, Zingg W, Neumann AW. Protein adsorption to polymer particles: role of surface properties. J Biomed Mater Res 1987;21:161–71.
[9] Haas TA, Plow EF. Integrin-ligand interactions: a year in review. Curr Opin Cell Biol 1994;6:656–62.
[10] Lyman S, Gilmore A, Burridge K, Gidwitz S. White GC 2nd integrin-mediated activation of focal adhesion kinase is independent of focal adhesion formation or integrin activation. Studies with activated and inhibitory beta3 cytoplasmic domain mutants. J Biol Chem 1997;272(36):22538–47.
[11] Gupta AK, Gupta M, Yarwood SJ, Curtis ASG. Effect of cellular uptake of gelatin nanoparticles on adhesion, morphology and cytoskeleton organisation of human fibroblasts. J Control Rel 2004;95(2):197–207.
[12] Gupta AK, Curtis ASG. Lactoferrin and ceruloplasmin derivatized superparamagnetic iron oxide nanoparticles for targeting cell surface receptors. Biomaterials 2004;25(15):3029–40.
[13] Gagesu R, Gruenberg J, Smyte E. Membrane dynamics in endocytosis: structure-function relationship. Traffic 2000;1: 84–8.
[14] Yang Y, Bauer C, Strasser G, Wollman R, Julien J-P, Fuchs E. Integrators of the cytoskeleton that stabilize microtubules. Cell 1999;98:229–38.
[15] Dewar H, Warren DT, Gardiner FC, Gourlay CG, Satish N, Richardson MR, Andrews PD, Ayscough KR. Novel proteins linking the actin cytoskeleton to the endocytic machinery in *Saccharomyces cerevisiae*. Mol Biol Cell 2002;13(10):3646–61.
[16] Yuen S. Pullulan and its applications. Process Biochem 1974; 9(9):7–9.
[17] Kaneo Y, Tanaka T, Nakano T, Yamaguchi Y. Evidence for receptor-mediated hepatic uptake of pullulan in rats. J Control Rel 2001;70(3):365–73.
[18] Gupta AK, Wells S. Surface modified superparamagnetic nanoparticles for drug delivery: preparation, characterisation and cytotoxicity studies. IEEE Trans Nanobiosci 2003;3(1):66–73.
[19] Adams PE. Determining iron content in foods by spectrophotometry. J Chem Ed 1995;72:649–51.
[20] Gupta AK, Curtis ASG. Surface modified superparamagnetic nanoparticles for drug delivery: interaction studies with human fibroblasts in culture. J Mater Sci: Mater Med 2004;15:493–6.
[21] Mosmann T. Rapid colorimetric assay for cellular growth and survival: application to proliferation and cytotoxic assay. J Immunol Methods 1993;95:55–63.
[22] Berry CC, Wells S, Charles S, Curtis ASG. Dextran and albumin derivatised iron oxide nanoparticles: influence on fibroblasts in vitro. Biomaterials 2003;24(25):4551–7.
[23] Gupta AK, Berry C, Gupta M, Curtis A. Receptor-mediated Targeting of magnetic nanoparticles using insulin as a surface ligand to prevent endocytosis. IEEE Trans Nanobiosci 2003; 2(4):256–61.
[24] Riezman H, Woodman PG, van Meer G, Marsh M. Molecular mechanisms of endocytosis. Cell 1997;91:731–8.
[25] Xi K, Tabata Y, Uno K, Yoshimoto M, Kishida T, Sokawa Y, Ikada Y. Liver Targeting of Interferon Through Pullulan Conjugation. Pharm Res 1996;13(12):1846–50.